Clays and Clay Minerals, Vol. 41, No. 6, 645–654, 1993.

THE FORMATION OF ILLITIC CLAYS FROM KAOLINITE IN KOH SOLUTION FROM 225°C TO 350°C

WUU-LIANG HUANG

Exxon Production Research Company, P.O. Box 2189
Houston, Texas 77252-2189

Abstract—Kaolinite was converted into illitic clays in a 2.58 m KOH solution in gold capsules using cold-seal pressure vessels at 225°, 250°, 300°, and 350°C and 500 bars. The XRD shows that the major reaction products are illitic clays with no interlayer expandability. The TEM shows that the illitic clays appear mainly platelet-like with a K/Si ratio close to that of muscovite/illite. The extent of the conversion was monitored by measuring the XRD peak ratio of muscovite (illite) and kaolinite in quenched run products. The results reveal that kaolinite converts to muscovite/illite in the KOH solution at an initial rate two to three orders of magnitude faster than that of similar reactions at near-neutral conditions.

Key words—Illite, Illite synthesis, Kaolinite, Kinetics.

INTRODUCTION

Studies of the paragenesis of authigenic illite in arkosic sandstones of various regions and ages have revealed that the illitization of kaolinite is an important reaction accounting for authigenic illite formation in sandstones during burial diagenesis (Hancock and Taylor, 1978; Sommer, 1978; Seemann, 1979; Rossel, 1982; Dutta, 1986). The equilibrium relationships of this reaction in arkosic sandstones have been previously studied (e.g., Bjorlykke, 1983). However, in low-temperature systems, reaction rates should be considered to determine the extent of illitization in arkosic sandstones, especially at shallow burial depths (Aagaard and Egeberg, 1987).

In addition to the experimental studies of the rate of illitization of smectite (Eberl and Hower, 1976; Howard and Roy, 1985; Whitney and Northrop, 1988; Huang *et al.*, 1993), the rate of illitization of kaolinite has recently been studied. Huang and Otten (1985) reported preliminary results on the kinetics of the kaolinite to K-mica conversion in alkaline solutions. Chermak and Rimstidt (1987 and 1990) experimentally determined the rate of kaolinite to muscovite/illite transformation in KCl solutions. Small (1993) measured the precipitation rate of illite from amorphous Al/Si gels. Huang (1992) experimentally simulated illite formation from a "model" arkosic sandstone containing kaolinite + feldspar + quartz with a variety of solution compositions. Velde (1965), in his study of muscovite polytype stabilities, demonstrated that muscovite can be synthesized very rapidly from kaolinite and KOH. The present study measures the rates for a similar reaction at lower temperatures. The results, when compared with those in near-neutral solutions, may shed light on the effect of pH on the kinetics of illite formation and place constraints on authigenic illite formation.

EXPERIMENTAL MATERIALS AND METHODS

Starting materials

The solid materials used were mainly synthetic kaolinite hydrothermally synthesized from glass at 300°C and 500 bars for six days in a Dickson-type pressure vessel (Seyfried *et al.*, 1979). The glass of kaolinite composition was prepared according to a standard method (Hamilton and Henderson, 1968) using tetraethylorthosilicate (TEOS) as a source of Si and aluminum nitrate for Al. A chemically homogeneous gel was first formed from the desired regent-grade chemicals; it was then fired at 800°C to form a glassy material. The synthetic kaolinite appears as pseudo-hexagonal platelets ranging from 0.1–2 μm with average grain size around 0.5 μm. Only those with diameters from 0.5–2 μm were used for the present experiments. The average surface area of the studied kaolinite measured by the BET method is 13.6 m^2/g. One experiment using the glass with kaolinite composition was also carried out. A 2.58 m (molality) KOH solution prepared using Baker-analyzed KOH was also used as a starting solution.

Experimental procedures

The hydrothermal experiments were carried out at 150°, 175°, 200°, 225°, 250°, 300° and 350°C in rapid-quench, cold-seal pressure vessels using gold capsules with dimensions of 0.44 cm O.D. × 1.9 cm length. Approximately 60 mg of kaolinite and 60 μl of the KOH solution were arc-sealed in the capsules. The bulk composition of the starting material in the capsules was equivalent to muscovite and water. However, the actual reaction equation or kinetic order cannot be obtained from this study because only one initial KOH concentration was used (Chermak, personal communication, 1993). The exact amounts of starting kaolinite

Table 1. Experimental results for conversion of kaolinite to illite with 2.58 m KOH solution at temperatures from 225°–350°C and 500 bars.

Run no.	Time (hours)	Reactants		Run products		
		Kaolinite (mg)	KOH soln (μl)	X-ray* peak ratio	Wt. % illite	X_{illite}
			350°C			
275	0.5	64.5	65.0	0.79	59	0.48
252	1.0	80.0	80.0	0.67	69	0.60
253	3.0	70.0	70.0	***	100	1.0
			300°C			
251	1	80.0	80.0	1.05	36	0.26
244	3	80.0	80.0	0.91	48	0.37
250	4.5	80.0	80.0	0.85	54	0.43
242	6	77.0	77.0	0.72	66	0.56
246	7.5	80.0	80.0	0.67	70	0.60
236	9	122	122	0.59	77	0.68
248	13	80.0	80.0	0.46	89	0.84
239	16	78.0	78.0	**	98	0.97
233	24	128	128	***	100	1.0
			250°C			
277	12	65.5	65.0	1.04	28	0.28
270	24	63.7	64.0	0.96	34	0.34
276	36	64.8	65.0	0.76	51	0.51
266	72	69.4	70.0	**	92	0.92
			225°C			
274	96	68.0	68.0	0.93	37	0.37
292	312	75.8	76.0	0.56	80	0.72

* See caption of Figure 1.
** Very weak kaolinite peaks.
*** No kaolinite peaks.
Additional runs at 300°C—run 229 (24 hr), run 230 (48 hr), and run 231 (1080 hr)—show complete conversion.

and solution for each individual run are listed in Table 1. The temperatures measured are precise to ±3°C and accurate to ±6°C. Some experiments, particularly those showing rapid reaction rates, were conducted using the "rapid-heating" method. The pressure vessel was preheated to a desired temperature, and then the gold capsule was dropped into the hot spot of the vessel so that the sample was rapidly heated to the run temperature within a few minutes. Each run was terminated by rapid quenching of the gold capsule. Details of product collection for solids and fluids are described in Huang *et al.* (1986) and Huang (1992). The solid products were routinely characterized by X-ray powder diffractometry (XRD), and selected ones were analyzed by scanning electron microscopy (SEM), analytical transmission electron microscopy (TEM), and thermogravimetric analysis (TGA).

Quantitative analysis of reaction progress

An XRD calibration curve was prepared from a series of mixtures containing various proportions of the starting kaolinite and a muscovite/illite that was prepared by complete conversion from kaolinite at 300°C for 24 hr. Sample preparation for XRD is critical in the quantification of results. Ten mg of each mixture were ultrasonically dispersed in 0.5 ml of distilled water. The water with clay suspension was dropped and confined in an area of 17 mm × 17 mm on a glass slide for air drying. The oriented clay film was used for XRD using CuKα radiation. The conventional calibration curve using the basal reflections of kaolinite and muscovite (7.14 Å and 10 Å, respectively) cannot be used because the d(001) 10 Å peak intensity of muscovite/illite is very weak (Figure 1A) due to the random arrangement of muscovite/illite platelets in the clay aggregates (Figure 4B). Two diagnostic peaks were chosen to measure quantitatively the relative amounts of kaolinite and muscovite/illite in the mixtures. A peak at 20.3° 2θ represents the combination of a major kaolinite reflection ($\bar{1}10$) at 4.361 Å and a minor muscovite/illite reflection (021) at 4.388 Å; whereas the peak at 19.9° 2θ is the combination of a major muscovite/illite reflection ($\bar{1}11$) at 4.448 Å and a minor kaolinite reflection (020) at 4.463 Å (Figure 1B). The calibration curve (Figure 2) shows a linear relationship between the peak height ratio and the relative quantities of kaolinite and muscovite/illite. A least-squares regression analysis gives the equation:

$$y = 1.442 - 0.011x,\ r^2 = 0.998$$

where y = peak height ratio (20.3°/19.9° 2θ), and x = weight percent of muscovite/illite clay in the kaolinite and muscovite/illite mixture. The relative uncertainty for measuring wt. % of muscovite/illite in the run products is considered to be ±10%.

The reaction products were prepared for XRD by using the described procedure. Provided that these two minerals are dominant in the products, the weight ratio can be used to follow the reaction progress that converts kaolinite to muscovite/illite. This is usually true for most experiments at temperatures higher than 225°C. XRD shows the presence of only kaolinite and muscovite/illite, and TEM indicates kaolinite + muscovite/illite and the presence of a trace amount of a third phase (boehmite or amorphous silica).

The precision of the XRD method was also confirmed independently by TGA analysis of products at 300°C (Table 2) with a Perkin Elmer TGS-2. A heating rate of 10°C/min was used. Data were analyzed with a Perkin-Elmer model 3600 data station. The calculation of the relative amounts of kaolinite and muscovite/illite from TGA data was based on the weight loss of water by assuming that only two minerals were present and that the muscovite/illite clay had a muscovite composition. Because of the difficulty in determining the beginning of dehydration of crystalline water, the TGA method is less accurate than the XRD method.

Electron microscopy

In addition to XRD analyses, the starting kaolinite and solid run products from experiments at 200° and

https://doi.org/10.1346/CCMN.1993.0410602 Published online by Cambridge University Press

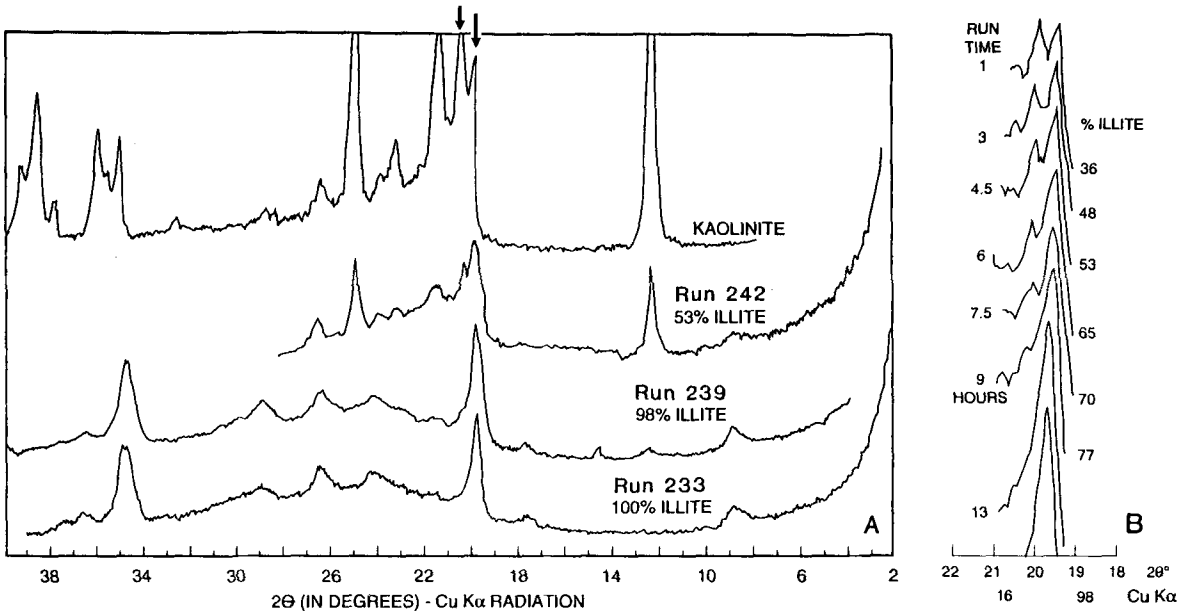

Figure 1. Typical X-ray patterns showing: A) starting kaolinite and run products for runs #242 (6 hr), #239 (16 hr) and #233 (24 hr) at 300°C; B) the progressive change of diagnostic X-ray peaks (marked by arrows in Figure 1A) as kaolinite converts into muscovite/illite at 300°C. The wt. % of muscovite/illite in kaolinite + muscovite/illite mixture is also shown next to the experimental run time.

300°C were selected for detailed analyses using SEM and TEM with selected area electron diffraction (SAD) and energy-dispersive X-ray spectroscopy (EDS) modes. The equipment, experimental procedures, and clay standards for chemical analysis are the same as those reported in Güven and Huang (1991).

RESULTS

Characteristics of starting kaolinite and reaction products

Microscopic characteristics of the starting kaolinite and the neoformed illitic clays are summarized in Table 3. The synthetic kaolinite appears mainly as pseudohexagonal platelets with an average grain size of 0.5 μm (Figure 3). Kaolinite also appears as dense aggregates of elongated and lath-like platelets which make up about 10–15% of the sample. The X-ray spectral data using TEM indicate that these elongated and lath-like platelets are kaolinite. No unreacted glass or other phase was found in the sample. Detailed microscopic characterization of the synthetic kaolinite was presented in Huang (1993).

Electron microscopic examination of the run products at 300°C (16 hr) reveals that the starting kaolinite platelets were first altered by the loss of their original pseudohexagonal form while illitic clays grew as short filaments or laths on the large rose-like kaolinite ag-

Table 2. Comparison of TGA and X-ray determinations of the percentage of illite and kaolinite present in the run products.

Run no.	Time (hours)	Wt. % loss (measured by TGA)	Wt. % of phases in run product*			
			TGA method		X-ray method	
			Illite	Kaolinite	Illite	Kaolinite
		300°C—500 bars				
251	1	11.9 ± 0.8	21	79	36	64
244	3	10.1 ± 0.6	40	60	48	52
242	6	6.8 ± 0.3	76	24	66	34
236	9	6.1 ± 0.3	83	17	77	23
239	16	4.9 ± 0.3	96	4	98	2
233	24	4.3 ± 0.3	100	0	100	0

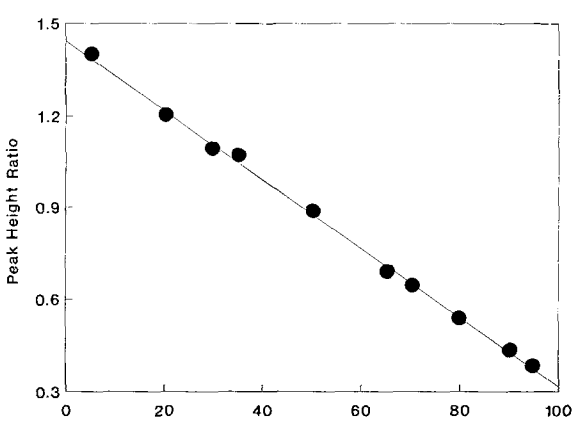

Figure 2. Calibration curve for determining wt. % of muscovite/illite in kaolinite and muscovite/illite mixture using XRD. Ordinate represents the peak height ratio 20.3°/19.9° 2θ.

https://doi.org/10.1346/CCMN.1993.0410602 Published online by Cambridge University Press

Table 3. TEM data of illitic clays, kaolinite, and minor phases from selected run products.

Run no.	Temp. (°C)	Time (hours)	Morphology illitic clays	SAD analysis or cell dimensions	EDS analyses atomic ratio	
					Al/Si	K/Si
239	300	16	hexagonal platelets	spot pattern on platelets	0.94	0.43
262	200	144	hexagonal platelets	2M stacking a = 5.21 ± 0.01 Å b = 8.97 ± 0.01 Å	0.4	0.12
			kaolinite platelets		0.86	0.05
			hexagonal boehmite platelets	a = 3.90 ± 0.02 Å c = 2.84 ± 0.01 Å		
284	200	600	platelets		0.68	0.33

gregates (Figure 4B). The unreacted kaolinite is composed of aggregates of extremely small platelets with some well-preserved hexagonal outlines (Figure 5D). A close view of illitic platelets shows a crystal mosaic composed of pseudohexagonal platelets (Figure 5A); most of the neoformed illitic platelets are about the size of the starting kaolinite platelets, and no continuous protective layer of illitic clays is present on the individual kaolinite platelets. The SAD pattern obtained from these platelets shows a spot pattern like a single platelet, indicating a strict crystallographic arrangement of these platelets. The EDS analysis of this type of platelet shows high Al and K contents, close to muscovite.

All illitic clays neoformed from kaolinite in the present experiments contain no detectable expandability based on XRD of glycolated samples. I use a general term "illitic clay" for the neoformed K-micas of a variety of compositions, including fine-grained muscovite, illite, and illite/smectite formed in the present experiments since they occur in clay-size (less than 4 μm) fractions (Środón and Eberl, 1984). However, for those formed at 225°C and above, the term "muscovite/illite" is used since their composition is close to muscovite.

In general, most illitic clays formed at 300°C show K/Si ratios close to that of muscovite. Some of the illitic clays formed at 200°C and below show a rather low K/Si ratio (Figures 4C, 4D, and 5B). The significant change of illitic clay composition corresponds to the appearance of K-natrolite (Figure 4A) and trace amounts of boehmite (Figure 5C) in the run product at 200°C and below.

Conversion rate of kaolinite to muscovite/illite

The data at 225°, 250°, 300°, and 350°C for the extents of kaolinite to muscovite/illite conversion as a function of run time, determined using XRD, are listed in Table 1. The quantification of the reaction progress using TGA method is also shown for comparison (Table 2). The results show that kaolinite converts progressively to muscovite/illite at all run temperatures. Examples of the X-ray patterns for runs at 300°C are presented in Figure 1B, which shows that the musco-

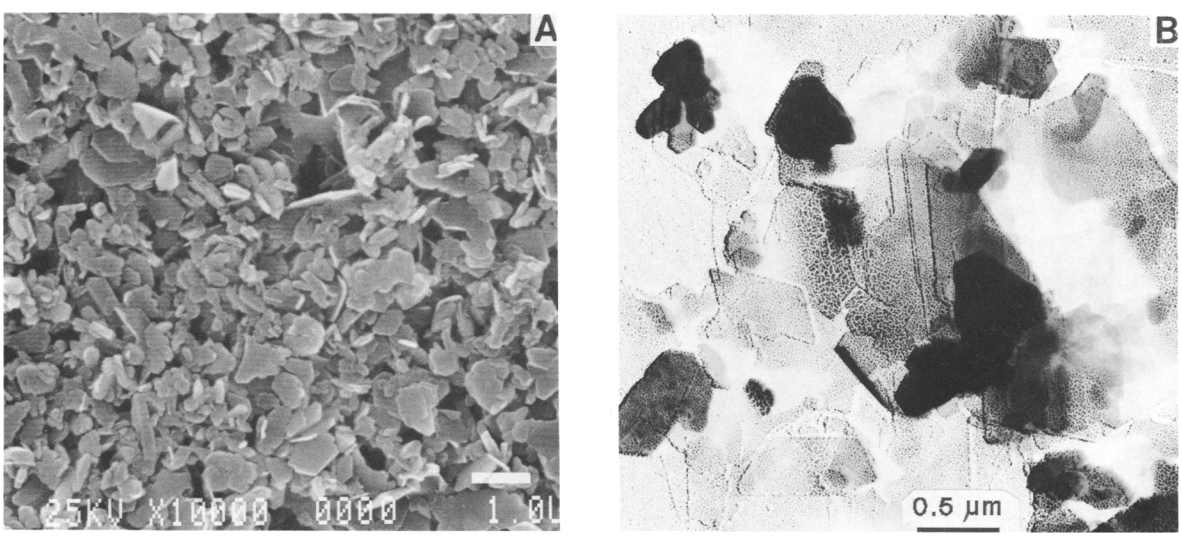

Figure 3. Electron micrographs of the synthetic kaolinite used in this study: A) SEM micrograph; and B) TEM micrograph.

https://doi.org/10.1346/CCMN.1993.0410602 Published online by Cambridge University Press

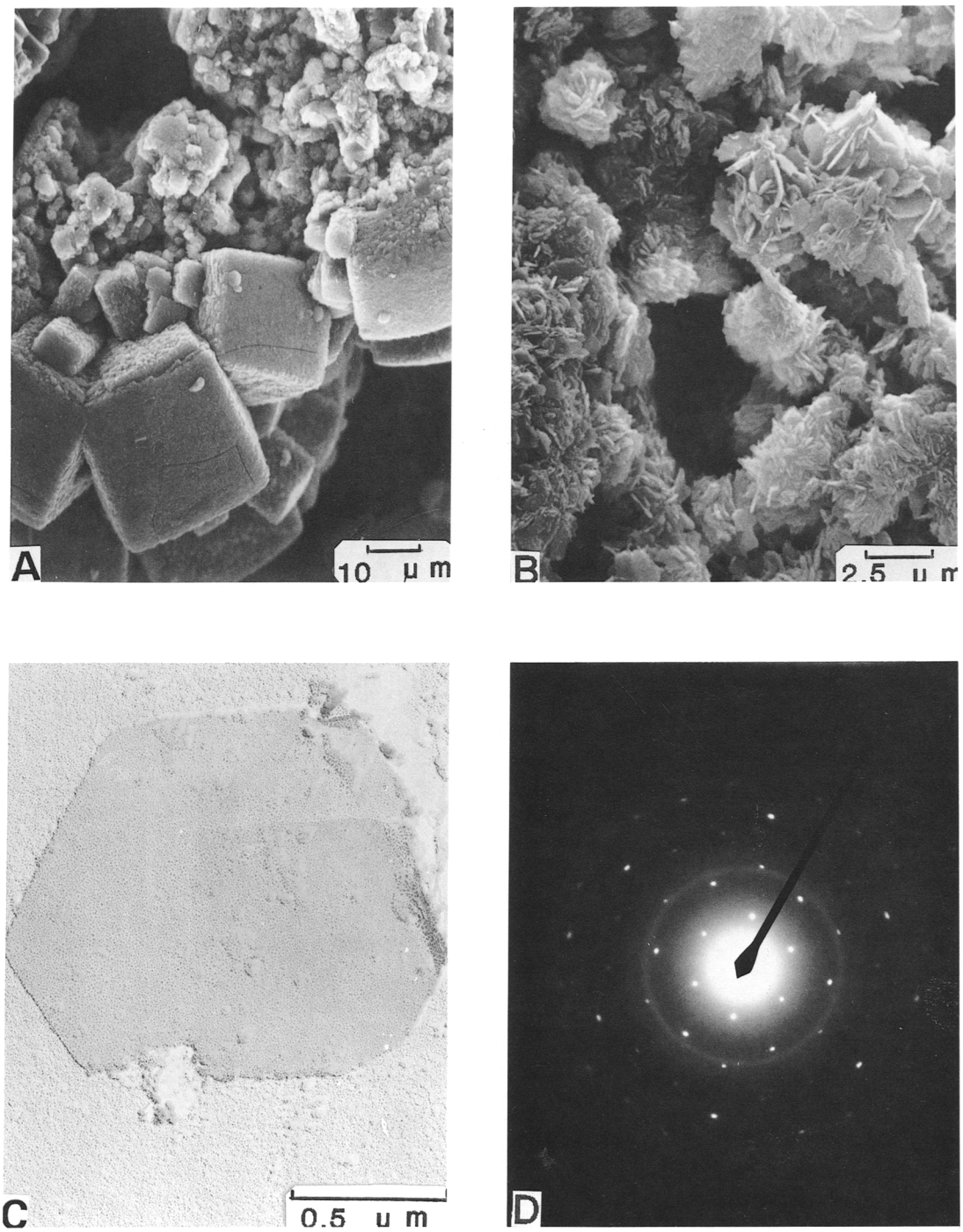

Figure 4. Electron micrographs of reaction products: A) K-natrolite precipitated at 200°C/6 days; B) aggregates of muscovite/illite platelets grown on the surface of kaolinite at 300°C/16 hr (run #239); C) illite or probably illite/smectite platelets neoformed at 200°C/6 days; and D) SAD pattern (cell dimensions shown in Table 3 obtained from the thin illitic platelet in Figure 4C).

vite (illite) peaks increase as the kaolinite peaks decrease with increasing run duration. The results also show that no significant incubation period is required for the conversion, although no muscovite/illite seed was added in the starting material. This suggests that the nucleation of muscovite/illite does not limit the conversion rate.

The reaction kinetics of kaolinite to muscovite/illite

https://doi.org/10.1346/CCMN.1993.0410602 Published online by Cambridge University Press

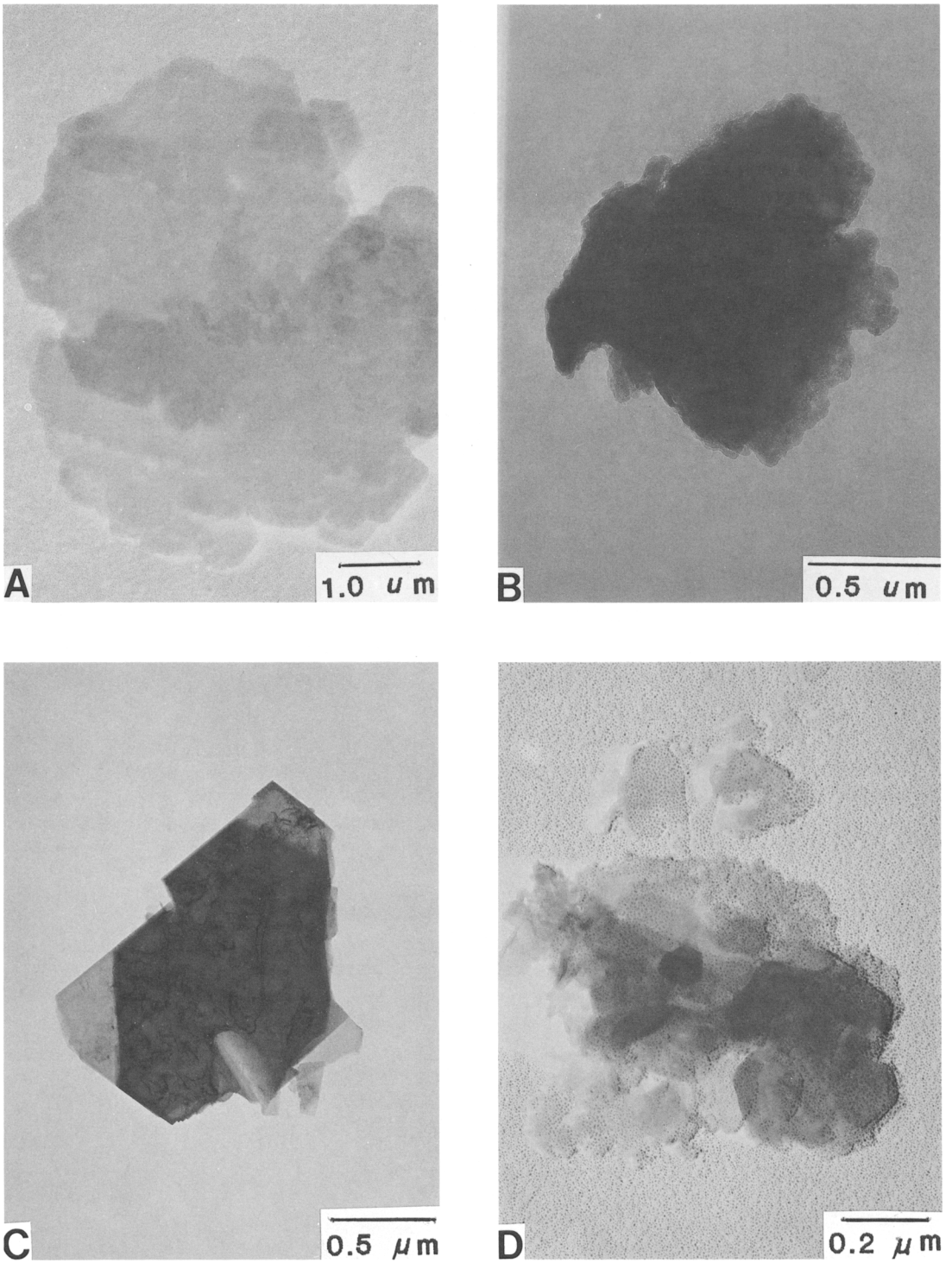

Figure 5. TEM micrographs of reaction products: A) a crystal mosaic that is made up of small (0.5 μm) pseudohexagonal platelets of muscovite/illite (300°C/16 h, run #239); B) aggregates (1–3 μm) with tiny irregular illitic platelets (150°C/150 days); C) hexagonal platelets of boehmite (200°C/6 days); and D) unreacted kaolinite composed of aggregates of extremely small platelets with some well-preserved hexagonal outlines (200°C/6 days).

https://doi.org/10.1346/CCMN.1993.0410602 Published online by Cambridge University Press

Table 4. The fitted polynomial equation for experimental data of fraction of illite formed *vs* time (in s).

225°C	
$X_{ill} = 1.26 \times 10^{-6}t - 5.52 \times 10^{-13}t^2$	$r^2 = 0.990$
250°C	
$X_{ill} = 0.034 + 4.15 \times 10^{-6}t - 3.00 \times 10^{-12}t^2$	$r^2 = 0.984$
300°C	
$X_{ill} = 0.094 + 2.36 \times 10^{-5}t - 1.52 \times 10^{-10}t^2$	$r^2 = 0.978$
350°C	
$X_{ill} = 0.035 + 2.22 \times 10^{-4}t - 1.25 \times 10^{-8}t^2$	$r^2 = 0.974$

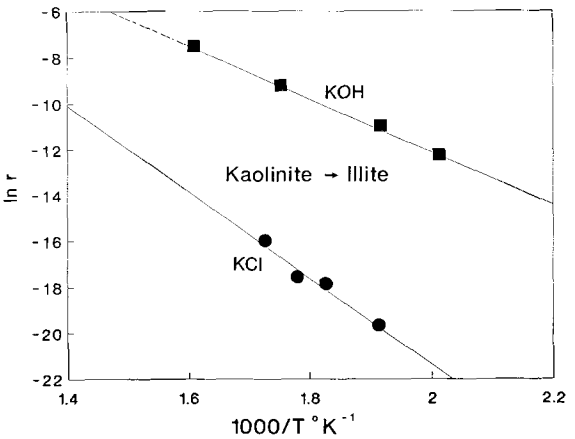

Figure 6. Comparison of Arrhenius plots showing the natural logarithm of initial rate ($r = dn_{H^+}/dt$ or dn_{ill}/dt in molal/s) *vs* 1000/T °K for the kinetics of kaolinite to muscovite/illite conversion in KOH (2.58 m) and in KCl solution (2 m) from Chermak and Rimstidt (1990). The activation energies calculated are, respectively, 104 kJ/mol and 157 kJ/mol in KOH and KCl solutions.

in KCl solution were found to be first order with respect to $[K^+]$ (Chermak and Rimstidt, 1990). For approximation, similar kinetic order is assumed in an alkaline KOH solution although the present experimental data are insufficient to confirm it. The assumed reaction can be written as:

$$1.5 \text{ kaolinite} + KOH = \text{muscovite} + 2.5\,H_2O \quad (1)$$

This assumption is reasonable since the composition of the illitic clay formed is close to muscovite and no solid phase other than kaolinite and muscovite/illite are present in the run product. The accurate determination of the reaction order requires experiments carried out at different concentrations of $[K^+]$.

The experimental results obtained at temperatures of 150°, 175° and 200°C, however, show that kaolinite first converted to illitic clay and K-natrolite and finally to illitic clay only as run time increased. The results show that within a few hours, at 200°C, about 40% of kaolinite decomposed to form both natrolite and illitic clay. This reaction seemed to stop for a long period of time before a rapid transformation of both kaolinite and natrolite to illitic clay occurred. No quantitative analysis of the reaction rate was performed for these runs.

DISCUSSION

Conversion rate

The experimental data for kaolinite to muscovite/illite conversion at 225°C and above was modeled using an initial rate method similar to that of Chermak and Rimstidt (1990). The data were polynomially fitted to an empirical equation for each temperature (Table 4). The initial and instant rates of conversion (dX_{ill}/dt) during the reaction were then calculated by differentiating the empirical equation for each temperature, where X_{ill} = the mole fraction of muscovite (illite) grown from kaolinite and t = time. The activation energy for the initial rate was calculated by applying the Arrhenius equation. The results are shown in Figure 6. An activation energy of 104 kJ/mol with an uncertainty of about ±20 kJ/mol can be calculated from the experimental data. The large uncertainty is due to the insufficient experimental data at temperatures other than 300°C.

It is interesting to note that the experimental data for the percent of conversion can also be fitted nicely ($r^2 = 0.98$) to a parabolic rate expression with:

$$X_{ill} = kt^{1/2} \quad (2)$$

where k is a temperature dependent rate constant. This model takes overall rates (not only the initial rate) into account and gives an activation energy of approximately 54 kJ/mol and a frequency factor approximately 137 (sec^{-1}). The parabolic rate implies a diffusion control (e.g., Wallast, 1967; Mathews, 1980). Because of the lack of experimentally observed protected layer on the kaolinite surface to support the diffusion mechanism, the model is less favorably considered for this reaction. However, the empirical Eq. 2 is useful for approximately modeling muscovite/illite formation in highly alkaline solutions (Huang, 1992).

The fast rate of kaolinite to muscovite/illite conversion in the KOH solution relative to that in neutral solutions, which will be discussed in the next section, was attributed by Velde (1965) to the rapid nucleation and growth of neoformed muscovite/illite, which inherits parts of the kaolinite structure. In order to evaluate this mechanism, an experiment using glass of kaolinite composition as starting material was also run at 300°C. The results show that there is no significant growth-rate difference between muscovite/illite formed from a crystalline kaolinite and that formed from glass of kaolinite composition. SEM observations also in-

https://doi.org/10.1346/CCMN.1993.0410602 Published online by Cambridge University Press

Table 5. Comparison of initial rates of kaolinite to illite conversion experimentally determined in KOH and KCl solutions.

KOH (2.58 m) (present study)			KCl (2.0 m) (Chermak and Rimstidt, 1990)		
Temp. (°C)	dX_{ill}/dt $\times 10^{-5}$	dm_{H+}/dt $(=dn_{ill}/dt)$ $\times 10^{-5}$	Temp. (°C)	dX_{ill}/dt $\times 10^{-8}$	dm_{H+}/dt $(=dn_{ill}/dt)$ $\times 10^{-8}$
225	0.126	0.49			
250	0.415	1.6	250	0.43	0.26
			275	2.77	1.72
			289	3.77	2.34
300	2.36	9.2			
			307	17.1	10.6
350	22.4	86.0			

Notes: dm_{H+}/dt is the initial rate in molal/s and is equal to dn_{ill}/dt in accordance with Eq. 1, where dn_{ill}/dt = mole of muscovite formed in mol/kg/s.

dX_{ill}/dt is the change rate of the mole fraction of muscovite in the mixture of kaolinite and muscovite in the solid run products and is equal to the rate of muscovite formed (mol/s) in the run product divided by the total moles of kaolinite and muscovite in the run product.

dn_{ill}/dt was converted into dX_{ill}/dt by multiplying a factor α. For the present experiments,

$$\alpha = 0.00006/\{(0.06/258)[(1 - \%\text{ kaolinite dissolved}) + (\%\text{ muscovite formed})]\}$$

where 0.00006 is the mass of water in kg in the run product, 0.06 is the weight of starting kaolinite in g, 258 is the formula weight of kaolinite, and % muscovite formed = (% kaolinite dissolved/1.5). At initial condition, $\alpha = 0.00006/(0.06/258) = 0.258$ for the present study and 1.61 for Chermak and Rimstidt (1990).

dicate that kaolinite extensively dissolves and loses most of its original shape. This suggests that the presence of an existing kaolinite layer is by no means a major factor accounting for the unusually fast conversion rate of kaolinite to muscovite/illite.

Comparison of rates in alkaline and neutral solution

For comparison, the initial rates reported by Chermak and Rimstidt (1990), based on the change of hydrogen ion concentration (dm_{H+}/dt) in near-neutral solutions during the kaolinite to muscovite/illite conversion, were recalculated to the conversion rates in mole fraction of illite formed in solids (dX_{ill}/dt) (Table 5). Conversely, the rate based on fraction of conversion monitored using solid run products in this study was also converted to the rate in dm_{H+}/dt assuming a stoichiometric relation of Eq. 1. The comparison shows that the initial reaction rate of kaolinite to muscovite/illite in the KOH solution is about two to three orders of magnitude higher than that in the KCl solution (Table 5 and Figure 6). The activation energy (104 kJ/mol) derived from the experiments in the alkaline solution is slightly lower than that (157 kJ/mol) derived from the neutral solution experiments reported by Chermak and Rimstidt (1990) (Figure 6).

The comparison was further performed by modeling the data at 300°C using the kinetic model of Chermak and Rimstidt (1990). The experimental data used for the model include the temperature, the K^+ and H^+ concentrations, the estimated surface areas of muscovite/illite (A_{ill}) in the run products, and mass (M) of water in the experimental solution. The decrease of $[K^+]$ and the increase of $[H^+]$ with run time were calculated using the initial solution concentrations and the extent of the reaction measured in each experiment assuming a stoichiometric relation of Eq. 1. The surface area of the run product was calculated using the average particle dimensions ($2.4 \times 1.6 \times 0.3\ \mu m$) of neoformed muscovite/illite estimated from microscopic data and the amount of muscovite/illite formed at a given time. The instant rates, dn_{ill}/dt (i.e., mole of muscovite/illite formed in 1 kg of water per second or dm_{H+}/dt) at different extents of reaction were first calculated using the kinetic model and later recalculated to the rate in dX_{ill}/dt for comparison (Table 6). The results show that the conversion rates calculated over a wide range of reaction extent are about 5 to 8 times slower than those experimentally observed (Table 6). The rate differences are much less pronounced than for the initial rate. This is attributed to the rapid decrease in solution pH because of low fluid rock ratio used as the reaction proceeds. The kinetic model of Chermak and Rimstidt (1990) derived from experiments in neutral solutions can better predict the present experimental data if solutions approach a near-neutral pH.

This big difference in initial rates between alkaline and near-neutral solutions, however, is not predicted from the previous kinetic model of Chermak and Rimstidt (1990). This suggests the reaction mechanism in alkaline solutions could be significantly different from that in near-neutral solutions.

CONCLUSIONS

Illitic clays with a variety of compositions have been grown from kaolinite in a KOH solution at elevated temperatures and pressures. Although no systematic compositional variation can be quantified from this study, the results show that most illitic clays formed at 300°C have K/Si ratios close to that of muscovite, whereas illitic clays formed at 200°C or below have composition similar to illite or mixed-layer illite/smectite. All illitic clays, however, show no detectable expandable layers by XRD. The morphology of most neoformed illitic clays is mainly platelet-like, subordinately lath-like, and rarely fibrous.

The present study also reveals that the solution pH significantly affects the kaolinite to muscovite/illite conversion rate. The conversion rate is about two to three orders of magnitude faster in an initially high alkaline solution than in near-neutral solution, whereas the activation energy in the KOH solution is slightly lower than that found in KCl solution. The unusually high conversion rate in the highly alkaline solution is

https://doi.org/10.1346/CCMN.1993.0410602 Published online by Cambridge University Press

Table 6. Calculation of kaolinite-to-illite conversion rate at 300°C based on experimental data of this study using the kinetic model of Chermak and Rimstidt (1990) by assuming first order kinetics.

Time (hours)	X_{ill} obs. frac.	m_{K^+} Molal	m_{H^+} Molal	A_{ill} (m^2)	M (kg × 10^{-3})	dn_{ill}/dt (mol/kg/s × 10^{-5})	dX_{ill}/dt (1/s × 10^{-6}) Calc.	dX_{ill}/dt (1/s × 10^{-6}) Obs.
0	0.00	2.58	1.23×10^{-11}	0	6			23.6
1	0.26	1.70	1.86×10^{-11}	0.14	6	1.09	3.18	22.6
3	0.37	1.37	2.32×10^{-11}	0.20	6	1.21	3.71	20.4
4.5	0.43	1.21	2.61×10^{-11}	0.22	6	1.21	3.80	18.7
6	0.56	0.87	3.62×10^{-11}	0.28	6	1.09	3.61	17.1
7.5	0.60	0.80	3.97×10^{-11}	0.29	6	1.04	3.48	15.4
9	0.68	0.62	5.13×10^{-11}	0.32	6	0.84	3.06	13.8
13	0.84	0.28	1.13×10^{-10}	0.37	6	0.47	1.73	9.4
16	0.97	0.05	6.63×10^{-10}	0.41	6	0.08	0.34	6.1

Notes: Frac. = fraction, m_{K^+} = molal of K^+, m_{H^+} = molal of hydrogen ion, A_{ill} = surface area of illite in run product, M = mass of solution, dn_{ill}/dt = rate of illite formed, calc. = calculated, obs. = observed, X_{ill} = mole fraction of illite, and dX_{ill}/dt = the rate of X_{ill} change.

m_{K^+} and m_{H^+} were calculated based on the extent of conversion using Eq. 1; A_{ill} was estimated using the observed particle size of neoformed illite; M was estimated from the volume of solution used.

dn_{ill}/dt was calculated based on the kinetic model of Chermak and Rimstidt (1990); the calculated dX_{ill}/dt was converted from dn_{ill}/dt (see note in Table 5); the observed dX_{ill}/dt is instant rate calculated using initial rate method.

not predicted from the previous kinetic model, experimentally derived from near-neutral KCl solutions. A systematic experimental program in the future using buffered solutions over a wide range of pH is required to quantify the effect of pH on the rates.

ACKNOWLEDGMENTS

The author would like to thank his colleagues G. A. Otten, A. M. Bishop, R. W. Brown, and J. A. Clouse for their assistance, respectively, in hydrothermal experiments, solution analyses, SEM examinations, and TGA analyses. The author's thanks are also extended to Professor N. Güven at Texas Tech University for help in TEM analyses and interpretations of selected run products. The review and comments of the early version by N. Güven, R. J. Pottorf, and G. Whitney are gratefully acknowledged. The critical review of late version and valuable suggestions on the reaction kinetics from J. A. Chermak have significantly improved the paper.

REFERENCES

Agaard, P. and Egeberg, P. K. (1987) Formation water chemistry in the late Triassic-Jurassic reservoirs offshore Norway (abs.): in *Prediction of Reservoir Quality through Chemical Modeling, Abstracts, AAPG Conference,* Park City, Utah.

Bjorlykke, K. (1983) Diagenetic reaction in sandstones: in *Sediments Diagenesis,* A. Parker and B. W. Shellwood, eds., Reidel Publishing Company, Boston, 169–213.

Chermak, J. A. and Rimstidt, J. D. (1987) Experimental determination of the rate of transformation of kaolinite to illite: *Abstracts with Program, Clay Minerals Society Annual Meeting,* Socorro, New Mexico, **24,** p. 46.

Chermak, J. A. and Rimstidt, J. D. (1990) The hydrothermal transformation of kaolinite to muscovite/illite: *Geochim. Cosmochim. Acta* **54,** 2979–2990.

Dutta, P. K. and Suttner, L. J. (1986) Alluvial sandstone composition and paleoclimate. II. Authigenic mineralogy: *J. Sed. Petrology* **56,** 346–358.

Eberl, D. D. and Hower, J. (1976) Kinetics of illite formation: *Bull. Geol. Soc. Amer.* **87,** 1326–1330.

Güven, N. and Huang, W. L. (1991) Effect of Mg^{2+} and Fe^{3+} substitutions on the hydrothermal illitization reactions: *Clays & Clay Minerals* **39,** 387–399.

Hancock, N. J. and Taylor, A. M. (1978) Clay mineral diagenesis and oil migration in the Middle Jurassic Brent Sand Formation: *Jour. Geol. Soc. London* **135,** 69–72.

Hamilton, D. L. and Henderson, C. M. B. (1968) The preparation of silicate composition by a gelling method: *Mineral. Mag.* **36,** 832–838.

Howard, J. J. and Roy, D. M. (1985) Development of layer charge and kinetics of experimental smectite alteration: *Clays & Clay Minerals* **33,** 81–88.

Huang, W. L. and Otten, G. A. (1985) Kinetics of K-mica and K-natrolite formation as a function of temperature: *Program and Abstracts, 2nd International Symposium on Hydrothermal Reactions,* University Park, Pennsylvania, p. 34.

Huang, W. L., Bishop, A. M., and Brown, R. W. (1986) Effect of fluid/rock ratio on albite dissolution and illite formation at reservoir conditions: *Clay Miner.* **21,** 585–601.

Huang, W. L. (1992) Illitic clay formation during experimental diagenesis of arkoses: in *Origin, Diagenesis, and Petrophysics of Clay Minerals in Sandstones,* D. W. Houseknecht and E. D. Pittman, eds., *SEPM. Spec. Publ.* **47,** 49–63.

Huang, W. L. (1993) Stability and kinetics of kaolinite to boehmite conversion under hydrothermal conditions: *Chem. Geol.* **105,** 197–214.

Huang, W. L., Longo, J. M., and Pevear, D. R. (1993) An experimentally derived kinetic model for smectite-to-illite conversion and its use as geothermometer: *Clays & Clay Minerals* **41,** 162–177.

Mathews, A. (1980) Influence of kinetics and mechanism in metamorphism: A study of albite crystallization: *Geochim. Cosmochim. Acta* **44,** 387–402.

Rossel, N. C. (1982) Clay mineral diagenesis in Rotliegend eolian sandstones of the southern North Sea: *Clay Miner.* **17,** 69–77.

Seeman, U. (1979) Diagenetically formed interstitial clay minerals as a factor in Rotliegend sandstone reservoir quality in the North Sea: *J. Petr. Geol.* **1,** 55–62.

Seyfried Jr., W. E., Gordon, P. C., and Dickson, F. W. (1979)

A new reaction cell for hydrothermal solution equipment: *Amer. Mineral.* **64,** 646–649.

Small, J. S. (1991) Experimental determination of the rates of precipitation of authigenic illite and kaolinite in the presence of aqueous oxalate and comparison to the K/Ar ages of authigenic illite in reservoir sandstones: *Clays & Clay Minerals* **41,** 191–208.

Sommer, F. (1978) Diagenesis of Jurassic sandstones in the Viking Graben: *J. Geol. Soc. London* **125,** 63–67.

Środón, J. and Eberl, D. D. (1984) Illite: in *Micas,* S. W. Bailey, ed., *Reviews in Mineralogy* **13,** 495–544.

Velde, B. (1965) Experimental determination of muscovite polymorph stabilities: *Amer. Mineral.* **50,** 436–449.

Wallast, R. (1967) Kinetics of the alteration of K-feldspar in buffered solutions at low temperature: *Geochim. Cosmochim. Acta* **31,** 635–648.

Whitney, G. and Northrop, H. R. (1988) Experimental investigation of the smectite to illite reaction: Dual reaction mechanisms and oxygen-isotope systematics: *Amer. Mineral.* **73,** 77–90.

(Received 19 March 1992; accepted 9 August 1993; Ms. 2199)